https://doi.org/10.5194/gmd-2019-264
Preprint. Discussion started: 17 October 2019

Geoscientific Model Development Discussions
Open Access

A computationally efficient model for probabilistic local warming projections constrained by history matching and pattern scaling

Philip Goodwin[1], Martin Leduc[2], Antti-Ilari Partanen[3], H. Damon Matthews[4] and Alex Rogers[5]

[1]School of Ocean and Earth Science, University of Southampton, Southampton, SO14 3ZH, UK
[2]Ouranos, Montreal, Canada
[3]Climate System Research, Finnish Meteorological Institute, Helsinki, Finland
[4]Department of Geography, Planning and Environment, Concordia University, Montreal, Canada
[5]Department of Computer Science, University of Oxford, Oxford, UK

Correspondence to: Philip Goodwin (p.a.goodwin@soton.ac.uk)

Abstract. Climate projections are made using a hierarchy of models of different complexities and computational efficiencies. While the most complex climate models contain the most detailed representations of many physical processes within the climate system, both parameter space exploration and Integrated Assessment Modelling require the increased computational efficiency of reduced-complexity models. This study presents an efficient model for projecting local warming across the globe, combining observation constrained global mean projections of an efficient Earth system model with spatial pattern scaling derived from the Climate Model Intercomparison Project phase 5 (CMIP5) ensemble. First, global mean warming is projected using a 10^3-member ensemble of history-matched simulations with the reduced complexity Warming Acidification and Sea-level Projector (WASP) Earth system model. The ensemble-projection of global mean warming from this WASP ensemble is then converted into local warming projections using a pattern scaling analysis from the CMIP5 archive, considering both the mean and uncertainty of the Local to Global Ratio of Temperature Change (LGRTC) spatial patterns from the CMIP5 ensemble for high-end and mitigated scenarios. The LGRTC spatial pattern does not appear strongly scenario dependent in the CMIP5 ensemble, and so should be useful across a variety of arbitrary scenarios. The computational efficiency of our WASP/LGRTC model approach makes it ideal for future incorporation into an Integrated Assessment Model framework, or efficient assessment of multiple scenarios. We utilise an emergent relationship between warming and future cumulative carbon emitted in our simulations to present an approximation tool making local warming projections from total future carbon emitted.

1 Introduction

The dominant climate projections, used by the 5th Assessment Report (AR5) of the Intergovernmental Panel on Climate Change (IPCC, 2013), are made using the Climate Model Inter-comparison Project phase 5 (CMIP5) ensemble (Taylor et al, 2012). However, due to their high level of complexity, state-of-the-art CMIP5 Earth System Models (ESMs) are computationally demanding, and thus cannot be used on a regular basis to inform decision makers about the impacts of arbitrary carbon-emission scenarios.

While a couple of years separate the different generations of CMIP-like experiments, many applications rather require climate simulations to be generated within a much shorter time frame. For instance, impact assessments may require climate projections for scenarios not considered by the CMIP5 experiments, for example scenarios designed to meet Paris Climate Agreement targets and maintain global mean surface warming below 1.5 or 2 °C (e.g. van Vuuren et al., 2018; Brown et al., 2018; Nicholls et al., 2018; Goodwin et al., 2018a), and physical climate simulations are required within Integrated Assessment Models exploring the coupled economic, societal, ecological and climate systems (e.g. van Vuuren et al., 2018; van Vuuren et al., 2017; McJeon et al., 2014).

https://doi.org/10.5194/gmd-2019-264
Preprint. Discussion started: 17 October 2019

To generate computationally efficient climate simulations, a range of lower-complexity – but numerically more efficient – climate models have been developed. They generally use a reduced spatial resolutionand/ora simplified representation of processes included within the complex models (e.g. Smith, 2012; Meinshausen et al., 2011a; Goodwin et al., 2018b).

For example, the highly efficient MAGICC6 climate model uses an upwelling-diffusion representation of the ocean and an hemispherical averaged spatial resolution (Meinshausen et al., 2011a). MAGICC6 has been configured to emulate an ensemble of the more complex Climate Model Intercomparison Project phase 3 (CMIP3) climate models (Meinshausen et al., 2011a; 2011b), but at a fraction of the computational expense. To generate spatial projections using MAGICC, a pattern scaling approach (e.g. Herger et al., 2015) is applied to emulate the spatial climate patterns from the CMIP3 models (e.g. Fordham et al. 2012): the regional climate SCENarioGENerator (SCENGEN). This MAGICC6 (and combined MAGICC6/SCENGEN) climate model is computationally efficient enough to usefully couple into Integrated Assessment Model (IAM) frameworks, including the IMAGE, MESSAGEframeworks (van Vuuren et al., 2017; McJeon et al., 2014). A key goal of IAMs is to explore consequences of the coupled human-climate system, through coupling representations of the physical climate system with the biosphere and human/society interactions, often including energy generation and land-use changes.

A recent study (Goodwin et al., 2018b) takes a different approach to making future projections of global mean surface warming, using the computationally efficient Warming Acidification and Sea-level Projector (WASP) climate model (Goodwin, 2016; Goodwin et al., 2017). In Goodwin et al. (2018b) the efficient WASP model is configured, not by tuning the parameters to emulate existing complex climate models (e.g. Meinshausen et al., 2011a; 2011b), but instead by history matching (Williamson et al., 2015) the efficient model to real world data. Goodwin et al. (2018b) first generate one hundred million (10^8) simulations using WASP, by varying the model properties with a Monte Carlo approach. This includes an input distribution for climate sensitivity drawn from geological evidence (PALEOSENS, 2012). These 10^8 simulations are then integrated from year 1765 to 2017, and each of them is checked against a set of historic observational reconstructions of surface warming (Hansen et al., 2010; Smith et al., 2008; Vose et al., 2012), ocean heat uptake (Levitus et al., 2012; Giese et al., 2011; Balmaseda et al., 2013; Good et al., 2013; Smith et al., 2015; Cheng et al., 2017) and carbon fluxes (IPCC, 2013; le Quéré et al., 2016). Only those WASP simulations that are consistent with the observational constraints are extracted to form the final history-matched ensemble of around $3{\times}10^4$ simulations (Goodwin et al., 2018b, see Supplementary Table 3 therein). This final history matched ensemble is then used to make future projections (Goodwin et al., 2018b). Note that the WASP ensemble is not configured to emulate the performance of more complex models, but to be consistent with observations of the real climate system.

The WASP model (Goodwin, 2016) produces projections for global mean surface warming only (Goodwin et al., 2018b), so to gain information to calculate local warming we here apply a pattern scaling tool. Leduc et al (2016) have recently shown that the spatial pattern of warming across CMIP5 models is relatively robust even though the average warming varies widely between ensemble members. Using the well-known pattern scaling approach (Tebaldi and Arblaster, 2014), Leduc et al. (2016) calculated the spatial pattern of the Local to Global Ratio of Temperature Change (LGRTC) that represented the CMIP5 ensemble, including both the mean and standard deviation in this spatial pattern.

Globally, the near-linear sensitivity of mean surface warming to cumulative carbon emissions is expressed via the Transient Climate Response to cumulative CO2 Emissions (TCRE in °C per 1000PgC), which is estimated to be in the range 0.8 to 2.5 °C per 1000PgC (IPCC, 2013; Matthews et al, 2009). One approach to generating local warming projections from carbon emission scenarios is to simply multiply the LGRTC characteristic of the CMIP5 ensemble (Leduc et al, 2016) by the

https://doi.org/10.5194/gmd-2019-264
Preprint. Discussion started: 17 October 2019

Geoscientific Model Development Discussions

estimated range for the TCRE and by the cumulative carbon emissions. However, this approach cannot be used to investigate or simulate several phenomena of potential interest. Firstly, the effective TCRE depends on the ratio of CO2 to non-CO2 radiative forcing (Williams et al. 2017a). Therefore, while the efficient climate models can be applied to investigate future warming for arbitrary scenarios, the TCRE cannot be applied unless it is for a scenario for which the TCRE is already estimated (e.g. Matthews et al. 2009; Williams et al., 2017a), for example the defined Representative Concentration Pathway (RCP) scenarios (Meinshausen et al. 2011c) or an idealised scenario with 1% per year increase in CO2 concentration (1pctCO2; Taylor et al, 2012) and no other forcing. Secondly, studies indicate that there can be a period of continued surface warming following cessation of annual carbon emissions (Frölicher et al., 2014; Williams et al., 2017b). This phenomenon cannot be explored using the TCRE alone, but is represented within efficient climate models such as WASP (Williams et al., 2017b). Thirdly, there is evidence that in some circumstances there is a path-dependence of surface warming from cumulative emissions (Zickfield et al, 2012), for example where cooling following negative emissions may not re-tracethe previous warming pathway. Again, this phenomenon is not captured within a constant TCRE framework, but may be explored with climate models. Thus a TCRE framework is applicable for certain situations, including idealised scenarios where the TRCE has already been established, but in the general case a time-dependent Earth system model is required.

In this study, we present a combined WASP/LGRTC Earth system model to generate computationally efficient local warming projections for arbitrary forcing scenarios. The combined WASP/LGRTC model makes local warming projections that are history matched to constrain the global mean surface warming (Goodwin et al., 2018b) and pattern scaled to the CMIP5 ensemble to generate the local information (Leduc et al., 2016). Our efficient model ensemble is able to produce warming-projections to year 2100 for arbitrary future carbon-emission scenarios in a matter of seconds on a standard desktop computer. An approximation tool is also presented making local warming projections based on future cumulative carbon emitted, for idealised scenarios where the TCRE has been pre-established.

Section 2 describes the spatial warming patterns analysed for RCP4.5 (Thomson et al., 2011) and RCP8.5 (Riahi et al., 2011) scenarios in 22 CMIP5 models, following the methodology of Leduc et al. (2016). Section 3 describes our methods for producing an ensemble of warming projections for any locality using the combined WASP/LGRTC Earth system model, while Section 4 presents the approximation approach for cases when the TCRE is pre-established. Section 5 discusses the wider implications of this study.

2. Spatial warming patterns in the CMIP5 ensemble for RCP4.5 and RCP8.5

Leduc et al (2016) demonstrated the utility of considering the spatial warming over time as a product of the global mean warming, $\Delta\overline{T}(t)$, and the spatial pattern of the Local to Global Ratio of Temperature Change, LGRTC(x,y), in the CMIP5 ensemble,

$$\Delta T(x, y, t) = \Delta\overline{T}(t) \times \mathrm{LGRTC}(x, y). \quad (1)$$

The mean and standard deviation in LGRTC were analysed across 12 CMIP5 models (Leduc et al, 2016), under a 1 per cent per year increase in atmospheric CO_2 concentration (1pctCO2; Taylor et al, 2012). To first order, the mean LGRTC can be treated as being independent of time and emission scenarios (Leduc et al, 2016, 2015).

Here, the spatial warming patterns in 22 CMIP5 models (see Supplementary Table S1) are examined for RCP4.5 (Thomson et al., 2011) and RCP8.5 (Riahi et al., 2011) scenarios that contain also non-CO2 forcings from for example anthropogenic non-CO2 greenhouse gas and aerosol emissions. We evaluated the LGRTC comparing mean global temperature between years 2006-2025 and 2079-2098.

Figure 1 shows the multi-model-mean LGRTC (μ_{LGRTC}) in RCP4.5 and RCP8.5 scenarios. With exception of oceanic regions where non-linear processes have important impacts on the climate sensitivity such like the sea-ice albedo feedback in the Arctic and the meridional overturning circulation in the north Atlantic (Leduc et al., 2016), LGRTC is very similar in both scenarios and also in the idealized 1pctCO2 scenario. The absolute value of differences in LGRTC between the three scenarios was below 0.72 °C per°C in all grid-cells and mostly below 0.2 °C per°C over the continents. Therefore, the choice of the emission scenario to define spatial pattern of warming in this study is not much relevant when only inhabited regions are considered.

Despite that the choice of the scenario has a relatively small impact on the warming patterns of interest here, it is worth noting that – in addition to the climate response to different radiative forcings – there are supplementary reasons explaining the previous differences. In particular, the differences in LGRTC between 1pctCO2 and the RCPs were caused by the lack of a clear basis for comparison: on the one hand, 1pctCO2 is an idealized scenario with no equivalent climatic states in the RCPs. For simplicity, we have chosen the preindustrial climate as the reference period in 1pctCO2 while in the RCP scenarios we used beginning of the 21st century. The end period was 20 years around the time of doubling of atmospheric CO2 concentration (70 years from the beginning) in 1pctCO2 and the years 2079-2098 in the RCPs. The different reference period meant that Arctic sea ice was already partly melted in the RCPs. This might have led to the large differences in the Arctic region, but detailed analysis and explanation is outside the scope of this study. Further differences between the 1pctCO2 scenario and the RCPs might have arisen from the different model ensemble. Both the different reference period and inclusion of non-CO2 forcers in RCP scenarios make the warming patterns from RCP scenarios more usable than those from the 1pctCO2 scenario to be used to predict warming patterns in the 21st century.

The uncertainty of the warming patterns, defined as standard deviation of LGRTC within the model ensemble (σ_{LGRTC}), was largest in the Arctic Ocean and in the Southern Ocean (Fig 2). Standard deviation was larger in the RCP4.5 than in RCP8.5 over most areas of the globe. Over continents, it was around 0.15-0.45 in RCP4.5 and mostly below 0.3 in RCP8.5.

3 Local warming projections in the pattern-scaled WASP/LGRTC ensemble

The aim here is to generate computationally efficient future projections of local warming across the globe, including a measure of the uncertainty in those local warming projections. This is distinct from generating a spatial warming projection that is internally physically consistent, maintaining physically plausible teleconnections between warming at different locations. Each CMIP5 model simulation creates a unique internally physically consistent spatial warming pattern for the prescribed forcing. When projecting local warming, including a measure of uncertainty, one method is to use information on the average and variation in the LGRTC information from multiple CMIP5 models (Figs. 1, 2). However, as soon as the information from multiple CMIP5 models are combined, the averaged result may not be internally physically consistent in terms of the spatial pattern of warming.

Section 3.1 describes how an observation-constrained projection of global mean surface warming is generated, including uncertainty. Section 3.2 then combines this global mean projection with the LGRTC information from the CMIP5 models (Section 2, above) to generate local warming projections.

https://doi.org/10.5194/gmd-2019-264
Preprint. Discussion started: 17 October 2019

Geoscientific Model Development
Discussions

3.1 Generating global mean warming projections

The WASP Earth system model comprises an 8-box representation of carbon and heat fluxes between the atmosphere, ocean and terrestrial systems (Goodwin, 2016), with surface warming solved via a functional equation linking warming to cumulative carbon emitted (Goodwin et al, 2015). For the terrestrial system, carbon uptake by photosynthesis is dependent on temperature and CO2, while carbon release via respiration is temperature dependent. Heat and carbon initially enters the ocean at the surface ocean mixed layer. Once in the surface ocean mixed layer, heat and carbon are exchanged with the sub-surface ocean regions over e-folding timescales that vary between each simulation in the ensemble.

Here, the WASP model configuration of Goodwin et al. (2018b) is used. First, WASP is used to generate 3×10^6 initial simulations in a Monte Carlo approach, each one integrated from years 1765 to 2017. A history matching approach (Williamson et al., 2015) is then adopted to assess these initial 3×10^6 simulations for observational consistency against historic warming, ocean heat uptake and carbon fluxes (Supplementary Table S2; and see Goodwin et al., 2018b for how the history matching approach is applied to the WASP model). A total of 1×10^3 simulations are found to be observationally consistent, such that their simulated values of surface warming, ocean heat uptake and carbon fluxes are consistent within observational uncertainty (Supplementary Table S2; Goodwin et al., 2018b).

The 1×10^3 observation-consistent simulations are extracted to form the final history matched ensemble. This ensemble is then integrated into the future to generate the distribution of global mean surface warming over time, (Figure 3). The distributions of global mean surface warming, $\Delta\overline{T_i}(t)$, projected by this configuration and history matching approach using the WASP ensemble, are similar to the CMIP5 projectionsfrom highly complex ESMs for the four RCP scenarios (Goodwin et al., 2018b, see figure 2 therein). However, possibly because the WASP projections are more tightly constrained to observations, they show reduced ensemble spread in future warming compared to the CMIP5 ensemble.

3.2 Generating local warming projections

We now utilise projected distributions from the same configuration of the WASP model to calculate distributions of local warming across the globe using the LGRTC pattern scaling approach of Leduc et al (2016). The aim is to generate an ensemble of projections of local warming at time t for a given RCP scenario, $\Delta T_i(x,y,t)$, by using the history matched WASP projections of $\Delta\overline{T_i}(t)$, and the mean and standard deviation of the LGRTC for the CMIP5 models, $\mu_{LGRTC}(x,y)$ and $\sigma_{LGRTC}(x,y)$ respectively (Figs 2-3).

For the ith ensemble member of this history matched WASP ensemble, the WASP/LGRTC projection of local warming at location x, y, $\Delta T_i(x,y,t)$, is constructed using both the mean and standard deviation in the LGRTC from the CMIP5 models,

$$\Delta T_i(x,y,t) = \Delta\overline{T_i}(t) \times [\mu_{LGRTC}(x,y) + z_i\sigma_{LGRTC}(x,y)]\ , \qquad (2)$$

where z_i is randomly chosen from a standard normal distribution. This distribution of local warming at time t, (eq. 2), includes both the uncertainty in global mean warming in the WASP ensemble (Figure 3; Goodwin et al., 2018b), and uncertainty in the spatial pattern of warming, σ_{LGRTC}, which is statistically derived from the CMIP5 ensemble (Figure 2; Leduc et al, 2016).

The full WASP/LGRTC-ensemble local warming projections for RCP 4.5 and RCP 8.5 are given in Fig. 4, which shows the mean, 17th and 83rd percentile of the warming across the globe from the 1×10^3 WASP/LGRTC ensemble members. To

https://doi.org/10.5194/gmd-2019-264
Preprint. Discussion started: 17 October 2019

Geoscientific Model Development Discussions

generate the local projections (eq. 2) for RCP4.5 and RCP8.5, we apply the pattern scaling analysed from the CMIP5 models for the appropriate scenario (Fig. 2). In both scenarios, there is more uncertainty, that is a higher range of responses between the 17th and 83th percentiles, in local warming at high northern latitudes (Fig. 4), consistent with this area showing a larger ensemble spread between CMIP5 models (Fig. 2).

The radiative forcing from aerosols can be highly localised, and so the ensemble mean and variation of local warming, $\mu_{LGRTC}(x,y)$ and $\sigma_{LGRTC}(x,y)$ in eq. (2), depends on how the CO_2 and non-CO_2 agents evolve in the scenario. For that reason, we include local warming patterns for the 1pctCO2 scenario as well as the RCP4.5 and RCP8.5 scenarios in the pattern scaling for the WASP/LGRTC model code (https://doi.org/10.5281/zenodo.3446023). This allows future users to choose the spatial pattern scaling that is most suitable for their scenario.

4. Approximation for arbitrary cumulative carbon emission scenarios

This section explores further increasing the computational efficiency for making spatial warming projections for idealised future scenarios, by approximating to the history matched WASP ensemble projections of global mean surface warming as function of cumulative carbon emitted after 2018, I_{em} in PgC.

The distribution of global mean surface warming in the WASP/LGRTC ensemble is approximately normally distributed for the RCP scenarios (Figure 3a). The history matched ensemble mean and standard deviation, $\mu_{\Delta\overline{T}}$ and $\sigma_{\Delta\overline{T}}$ respectively, are both well approximated by second order polynomials in cumulative carbon emitted (Figure 3b,c). The ensemble mean warming projections is given by,

$$\mu_{\Delta\overline{T}}(I_{em}) = a_1 I_{em}^2 + b_1 I_{em} + c_1\ , \qquad (3)$$

and the ensemble standard deviation by,

$$\sigma_{\Delta\overline{T}}(I_{em}) = a_2 I_{em}^2 + b_2 I_{em} + c_2\ , \qquad (4)$$

where a_1=3.50257×10^{-7}, b_1=2.50924×10^{-3} , c_1= 1.02159, a_2= 2.14129×10^{-8}, b_2=2.28077×10^{-4} and c_2=8.79361×10^{-2} for RCP8.5. Both the RCP4.5 and RCP2.6 scenarios see very similar warming per unit future carbon emitted to RCP8.5, while the RCP6.0 scenario sees only slightly less warming per unit future carbon emitted (Figure 4b,c).

Therefore, for emission scenarios over the 21st century in which the ratio of radiative forcing from sources other than CO2 to cumulative carbon emitted during the 21st century lies within the range of the RCP scenarios, the distribution of global mean surface warming from the history matched WASP ensemble can be approximated by quadratics in future carbon emitted (eqs. 3 and 4; Fig. 3)

The mean warming at location x,y is calculated by simply multiplying the mean of the 1×10^3 WASP ensemble members of the global average warming by the CMIP5 mean of the LGRTC,

$$\mu_{\Delta T}(x,y,I_{em}) = \mu_{\Delta\overline{T}}(I_{em}) \times \mu_{\mathrm{LGRTC}}(x,y)\ . \qquad (5)$$

https://doi.org/10.5194/gmd-2019-264
Preprint. Discussion started: 17 October 2019

The standard deviation in local warming at location *x,y* after cumulative emissions I_{em}, $\sigma_{\Delta T}(x, y, I_{em})$, is then calculated from the standard deviation in the global average warming in the *i* ensemble members, $\sigma_{\Delta \bar{T}}(I_{em})$, and the standard deviation in the LGRTC, $\sigma_{LGRTC}(x,y)$, using,

$$\sigma_{\Delta T}(x, y, I_{em}) = \mu_{\Delta T}(x, y, I_{em}) \sqrt{\left(\frac{\sigma_{\Delta \bar{T}}(I_{em})}{\mu_{\Delta \bar{T}}(I_{em})}\right)^2 + \left(\frac{\sigma_{\mathrm{LGRTC}}(x,y)}{\mu_{\mathrm{LGRTC}}(x,y)}\right)^2}. \quad (6)$$

Applying equations (5) and (6) provides a method to approximate local warming projections as a function of the future carbon emitted after the start of 2018 (Figure 5a; code available at https://doi.org/10.5281/zenodo.3446023), including uncertainty in the warming at any location (Figure 5b). This method assumes idealised future pathways within the range of the RCP2.6, RCP4.5 and RCP8.5 scenarios (Figure 3b,c), including a similar ratio of CO2 to non-CO2 radiative forcing. While this approximation tool (Fig. 5; eqs. 3-6) is not as general as the full WASP/LGRTC Earth system model in its potential applications, we anticipate it will still be a useful tool for user-friendly back-of-the-envelope approximations and pedagogical applications.

5. Discussion

A highly computationally efficient Earth System Model has been presented for projecting local warming projections, based on a history matched global mean warming projection using an efficient ESM (Goodwin, 2016; Goodwin et al., 2018b) and pattern scaling of the CMIP5 ensemble (Leduc et al., 2016): the WASP/LGRTC model. Along with the full WASP/LGRTC model is an easy to use normal error propagation approximation variant producing projected ranges of both global mean warming and the spatial distribution of warming for future cumulative carbon-emission values.

The WASP/LGRTC model presented here is an alternative to existing efficient climate models. For example, the MAGICC6/SCENGEN efficient model is often configured as an 'emulator' of the CMIP3 ensemble (Meinshausen et al, 2001a,b): the MAGICC6/SCENGEN model parameters are tuned such that the ensemble members emulate the properties of the more complex CMIP3 models in both global mean warming and spatial warming patterns. However, even the most complex of climate model ensembles show discrepancy to observations (Goodwin et al, 2018b), and this discrepancy will be reproduced by an emulating ensemble. In contrast, the WASP/LGRTC model is not tuned to emulate more complex models. Instead the WASP model parameters are empirically constrained using the observed histories of warming, heat uptake and carbon fluxes to generate global mean surface warming projections (Goodwin et al, 2018b). Meanwhile, the LGRTC spatial pattern applies the mean and standard deviation in the spatial warming from across the CMIP5 ensemble (Leduc et al, 2016), but does not seek to emulate any specific CMIP5 model within any specific WASP/LGRTC ensemble member.

At present, the WASP model requires prescribed radiative forcing from greenhouse gasses and agents other than CO2, for example methane or aerosols (Goodwin, 2016; Goodwin et al, 2018b). Future work will seek to implement an emission-based representation of other significant greenhouse gases and aerosols, allowing the WASP/LGRTC model to explore a wider range of future scenarios.

Both the WASP/LGRTC model and the quadratic approximation to WASP/LGRTC model are easy to use. The full WASP/LGRTC model can quickly generate output for arbitrary future scenarios, while the approximated model makes projections for different future cumulative emissions assuming that the relative CO2 and non-CO2 radiative forcing is in the range of the RCP8.5, RCP4.5 or RCP2.6 scenarios (Figure 3b,c compare black dashed line to red, orange and purple).

https://doi.org/10.5194/gmd-2019-264
Preprint. Discussion started: 17 October 2019

We anticipate that our full and approximated models will be beneficial both for scientific and pedagogical applications, where available computational resources or climate-model expertise exclude the use of highly complex models

Code availability. Versions of the WASP model is available from the public GitHub repository at https://github.com/WASP-ESM/WASP_Earth_System_Model. The specific code for both the WASP/LGRTC combined model approach used in this study, and the local warming projection approximation tool, are archived on Zenodo (https://doi.org/10.5281/zenodo.3446023).

Author Contributions. PG conducted the numerical modelling and coded the WASP/LGRTC model and approximation tool, with input from AR. AIP, MD and HDM analysed the spatial patterns in the CMIP5 models, and supplied the spatial arrays used by the WASP/LGRTC model and approximation tool. All authors contributed to writing the manuscript.

Competing interests. Authors declare no competing interests

Acknowledgements. PG acknowledges funding from UK NERC grant NE/N009789/1 and combined UK Government Department of BEIS and UK NERC grant NE/P01495X/1. ML thanks Ouranos and Concordia University. AIP was supported by Emil Aaltonen Foundation, The Fonds de recherche du Quebec - Nature et technologies (grant number: 200414), Concordia Institute for Water, Energy and Sustainable Systems (CIWESS), and Academy of Finland (grant number: 308365). We acknowledge the World Climate Research Programme's Working Group on Coupled Modelling, which is responsible for CMIP, and we thank the climate modelling groups (listed in Supplementary Table S1) for producing and making available their model output. For CMIP the U.S. Department of Energy's Program for Climate Model Diagnosis and Intercomparison provides coordinating support and led development of software infrastructure in partnership with the Global Organization for Earth System Science Portals.

References

Balmaseda, M. A., Mogensen, K.. and Weaver, A. T.: Evaluation of the ECMWF ocean reanalysis system ORAS4. Q. J. Roy. Meteorol. Soc. 139, 1132–1161, 2013.

Brown, S., R. Nicholls, P. Goodwin, I. Haigh, D. Lincke, A. Vafeidis, J. Hinkel: Quantifying Land and People Exposed to Sea-Level Rise with No Mitigation and 1.5 and 2.0 °C Rise in Global Temperatures to Year 2300, Earth's Future, doi:10.1002/2017EF000738, 2018.

Cheng, L. et al.: Improved estimates of ocean heat content from 1960 to 2015. Sci. Adv. 3, e1601545, 2017.

Fordham, D.A., Wigley, T.M.L., Watts, M.J., and Brook, B.W.: Strengthening forecasts of climate change impacts with multi-model ensemble averaged projections using MAGICC/SCENGEN 5.3, Ecography 35, 4-8, doi:10.1111/j.1600-0587.2011.07398.x, 2012.

Frölicher, T. L., Winton, M., and Sarmiento, J. L.: Continued global warming after CO2 emissions stoppage. Nature Climate Change, 4, 40–44, 2014

Giese, B. S., and Ray, S.: El Niño variability in simple ocean data assimilation (SODA), 1871–2008. J. Geophys. Res. 116, C02024, 2011.

Good, S. A., Martin, M. J., and Rayner, N. A.: EN4: quality controlled ocean temperature and salinity profiles and monthly objective analyses with uncertainty estimates. J. Geophys. Res. Ocean. 118, 6704–6716, 2013.

Goodwin, P., Brown, S., Haigh, I. Nicholls, R., and Matter, J.: Adjusting Mitigation Pathways to stabilize climate at 1.5 and 2.0 °C rise in global temperatures to year 2300, Earth's Future, doi:10.1002/2017EF000732, 2018a.

Goodwin. P., Katavouta, A., Roussenov, V.M., Foster, G.L., Rohling, E.J. and Williams, R.G.: Pathways to 1.5 and 2 °C warming based on observational and geological constraints, Nature Geoscience, doi:10.1038/s41561-017-0054-8, 2018b.

Goodwin, P.: How historic simulation-observation discrepancy affects future warming projections in a very large model ensemble, Climate Dynamics, doi:10.1007/s00382-015-2960-z, 2016.

Goodwin, P., Williams, R.G., and A. Ridgwell, A.: Sensitivity of climate to cumulative carbon emissions due to compensation of ocean heat and carbon uptake, Nature Geoscience, 8, 29-34, 2015.

Hansen, J., Ruedy, S., Sato, M., and Lo, K.: Global surface temperature change. Rev. Geophys. 48, RG4004, 2010.

Herger, N., Sanderson, B.M., and Knutti, R.: Improved pattern scaling approaches for the use in climate impact studies, Geophys. Res. Lett., 42, 3486 3494, doi:10.1002/2015GL063569, 2015.

IPCC Climate Change 2013: The Physical Science Basis (eds Stocker, T. F. et al.) (Cambridge Univ. Press, Cambridge, 2013).

Leduc, M., Matthews, H. D., and de Elía, R.: Quantifying the limits of a linear temperature response to cumulative CO2 emissions. Journal of Climate, 28(24), 9955–9968, 2015.

Leduc, M., Matthews, H.D., and de Elía, R.: Regional estimates of the transient climate response to cumulative CO2 emissions, Nature Climate Change, doi:10.1038/nclimate2913, 2016.

le Quéré, C. et al. Global carbon budget 2016. Earth Syst. Sci. Data 8, 605–649. 2016.

Levitus, S. et al.: World ocean heat content and thermosteric sea level change (0–2000 m), 1955–2010. Geophys. Res. Lett. 39, 10, 2012.

Matthews, H. D., Gillet, N. P., Stott, P. A., and Zickfield, K.: The proportionality of global warming to cumulative carbon emissions. Nature 459, 829–832.https://doi.org/10.1038/nature08047, 2009.

McJeon, H. et al.: Limited impact on decadal-scale climate change from increased use of natural gas, Nature 514, 482–485, doi:10.1038/nature13837, 2014.

Meinshausen, M., Raper, S.C.B., and Wigley, T.M.L.: Emulating coupled atmosphere-ocean and carbon cycle models with a simpler model, MAGICC6 – Part 1: Model description and calibration. Atmos. Chem. Phys. 11, 1417-1456, doi:10.5194/acp-11-1417-2011, 2011a.

Meinshausen, M., Raper, S.C.B., and Wigley, T.M.L.: Emulating coupled atmosphere-ocean and carbon cycle models with a simpler model, MAGICC6 – Part 2: Applications. Atmos. Chem. Phys. 11, 1457-1471, doi:10.5194/acp-11-1457-2011, 2011b.

Meinshausen, M. et al.: The RCP greenhouse gas concentrations and their extensions from 1765 to 2300. Climatic Change, 109, 213-241, 2011c.

Nicholls, R.J., Brown, S., Goodwin, P., Wahl, T., Lowe,T.J., Solan, M., Godbold, J.A., Haigh, I.D., Lincke, D., Hinkel, J., Wolff, C., and Merkens, J-L.: Stabilisation of global temperature at 1.5°C and 2.0°C: Implications for coastal areas, Philosophical Transactions of the Royal Society A. doi:10.1098/rsta.2016.0448, 2018.

PANAEOSENS project group members: Making sense of palaeoclimate sensitivity, Nature 491, 683-691, 2012.

Riahi, K., Rao, S., Krey, V., Cho, C., Chirkov, V., Fischer, G., Kindermann, G., Nakicenovic, N., and Rafaj, P.: RCP 8.5—A scenario of comparatively high greenhouse gas emissions, Climatic Change, 109,33–57, 2011.

Smith, D. M. et al.: Earth's energy imbalance since 1960 in observations and CMIP5 models. Geophys. Res. Lett. 42.4, 1205–1213, 2015.

Smith, R.S.: The FAMOUS climate model (versions XFXWM and XFHCC): description and update to version XDBUA, Geosci. Model Dev., 5, 269-276, doi:10.5194/gmd-5-269-2012, 2012.

Smith, T. M., Reynolds, R. W., Peterson, T. C., and Lawrimore, J.: Improvements to NOAA's historical merged land–ocean surface temperature analysis (1880–2006). J. Clim. 21, 2283–2296, 2008.

Taylor, K. E., Stouffer, R.J., and Meehl, G.A.: An overview of CMIP5 and the experiment design, Bulletin of the American Meteorological Society, 93, 485-498, doi:10.1175/BAMS-D-11-00094.1, 2012.

Tebaldi, C., & Arblaster, J.M.: Pattern Scaling: Its Strengths and Limitations, and an Update on the Latest Model Simulations, *Climatic Change*, 122(3), 459–471 (2014). http://dx.doi.org/10.1007/s10584-013-1032-9 .

Thomson, A. M., et al.: RCP4.5: A pathway for stabilization of radiative forcing by 2100, Climatic Change, 109(1), 77–94, doi:10.1007/ s10584-011-0151-4, 2011.

Williams, R.G, Goodwin, P., Roussenov, V.M., and Bopp, L.: A framework to understand the transient climate response to emissions. Environmental Research Letters, 11, doi:10.1088/1748-9326/11/1/015003, 2016.

https://doi.org/10.5194/gmd-2019-264
Preprint. Discussion started: 17 October 2019

Geoscientific Model Development Discussions

Williams, R.G., Roussenov, V., Goodwin, P., Resplandy, L., and Bopp, L.: Sensitivity of global warming to carbon emissions: effects of heat and carbon uptake in a suite of Earth system models, Journal of Climate 30, 9343-9363,doi:10.1175/JCLI-D-16-0468.1, 2017a.

Williams, R.G., Roussenov, V., Frölicher, T.L., and Goodwin, P.:, Drivers of continued surface warming after cessation of carbon emissions, Geophysical Research Letters 44, 10633-10642, GRL56532, doi:10.1002/2017GL075080, 2017b.

Williamson, D., Blaker, A. T., Hampton, C., and Salter, J.: Identifying and removing structural biases in climate models with history matching. Climate Dynamics 45, 1299, 2015.

van Vuuren D. P. et al.: Energy, land-use and greenhouse gas emissions trajectories under a green growth paradigm, Global Environmental Change 42, 237–250, doi:10.1016/j.gloenvcha.2016.05.008, 2017.

van Vuuren, D.P. et al.: Alternative pathways to the 1.5 °C target reduce the need for negative emission technologies, Nature Climate Change, doi:10.1038/s41558-018-0119-8, 2018.

Vose, R. S. et al.: NOAA's merged land–ocean surface temperature analysis. Bull. Am. Meteorol. Soc. 93, 1677–1685, 2012.

Zickfeld, K., Arora, V.K., and Gillett, N.P.: Is the climate response to CO2 emissions path dependent? Geophys. Res. Lett, 39, L05 703, 2012.

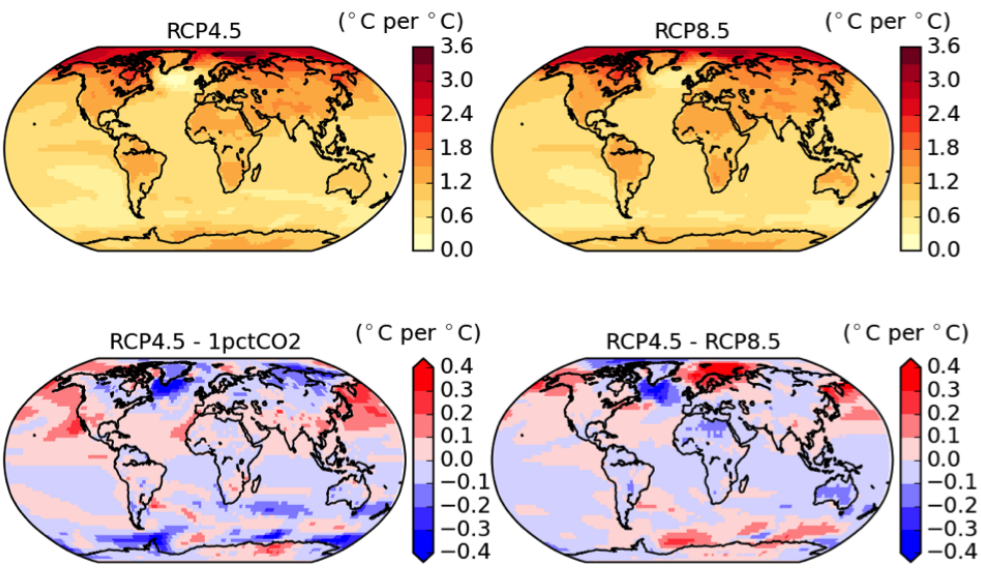

Figure 1: LGRTC in RCP4.5 and RCP8.5 from the analysed CMIP5 models, and differences in LGRTC between RCP4.5 and 1pct and between RCP4.5 and RCP8.5 scenarios.

Geoscientific Model Development
Discussions
Open Access

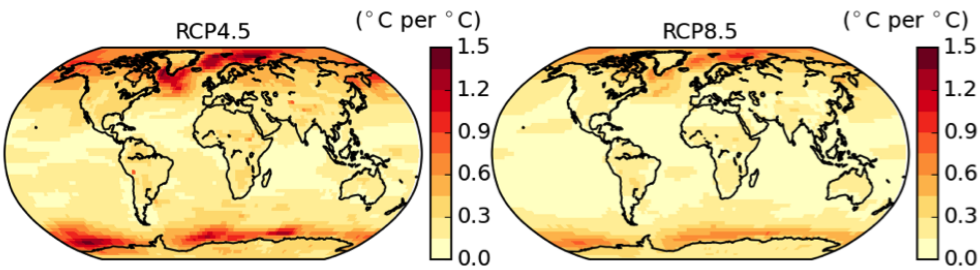

Figure 2: Standard deviation of LGRTC in the analysed CMIP5 models.

https://doi.org/10.5194/gmd-2019-264
Preprint. Discussion started: 17 October 2019

Geoscientific Model Development
Discussions

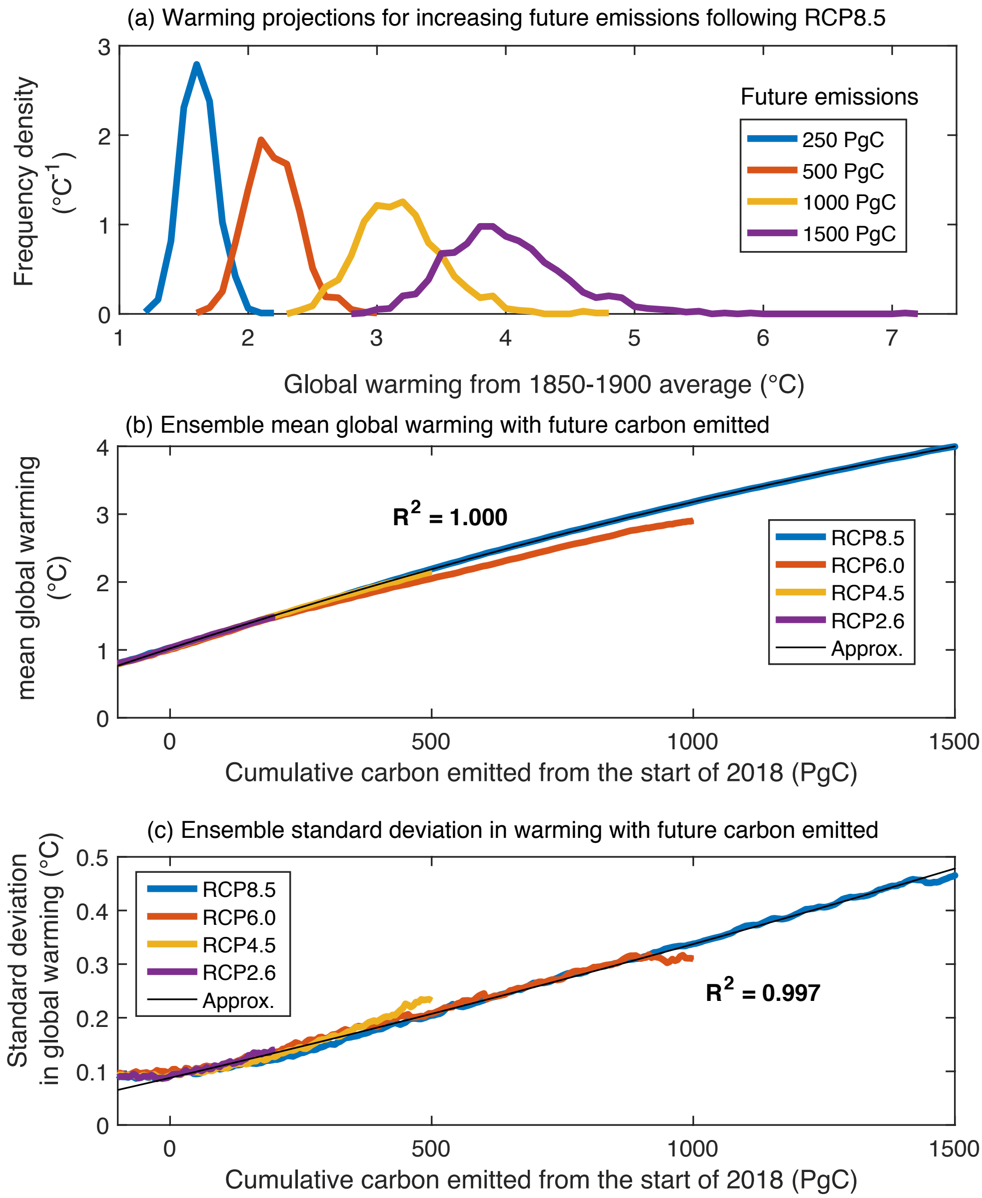

Figure 3: Projections of global mean surface warming from the history matched WASP ensemble for different future carbon emission sizes. (a) Frequency distributions of projected warming in the WASP ensemble for different future carbon emission sizes after the start of 2018. (b) Ensemble-mean global warming as future cumulative carbon emitted increases. (c) Ensemble standard deviation in global warming as future carbon emitted increases. (b) and (c) show the RCP8.5 (blue), RCP6.0 (red), RCP4.5 (orange) and RCP2.6 (purple) scenarios. A quadratic approximation, eq. 3 for (b) and eq. 4 for (c), is a good fit to the RCP8.5 scenario (thin black line). All panels show warming calculated relative to the 1850-1900 average.

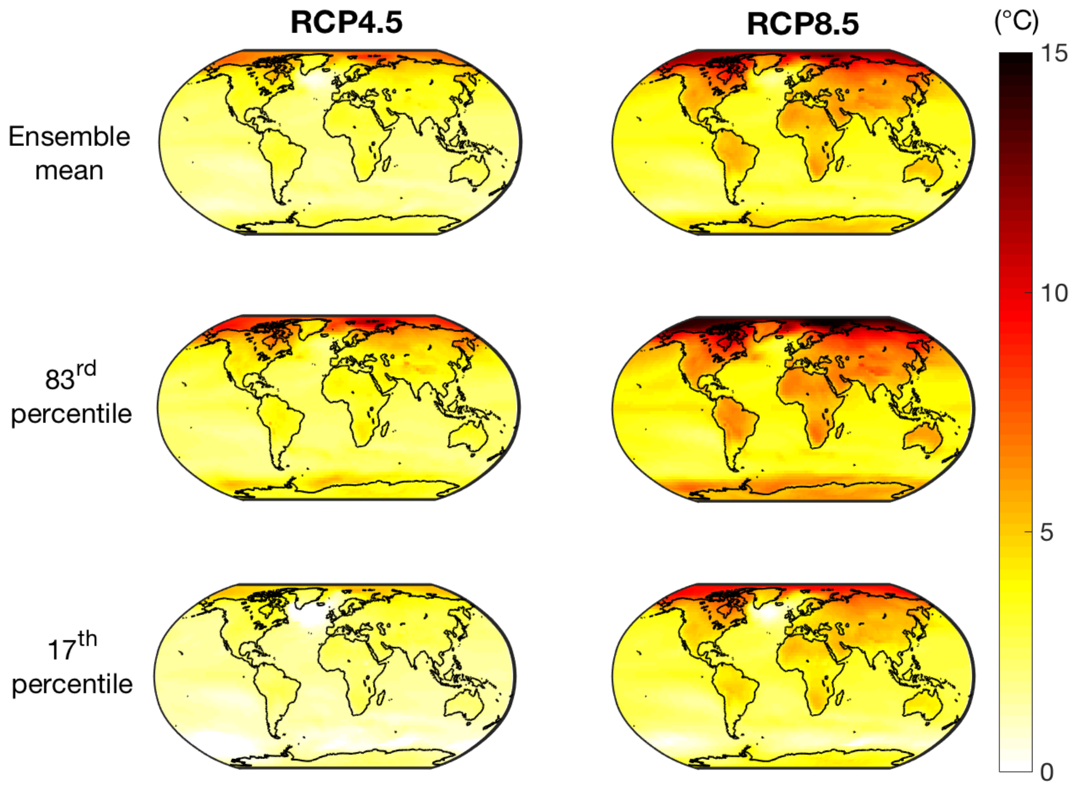

Figure 4: Projected warming for the period 2081-2100 relative to the 1850-1900 average from 1×10^3 history matched simulations of the ultra-fast WASP/LGRTC ensemble. The left-hand column is for the RCP4.5 scenario and the right-hand column is for the RCP8.5 scenario. The top, middle and bottom rows represent the mean, 83rd percentile and 17th percentile of the model ensemble.

https://doi.org/10.5194/gmd-2019-264
Preprint. Discussion started: 17 October 2019

Geoscientific Model Development Discussions
Open Access

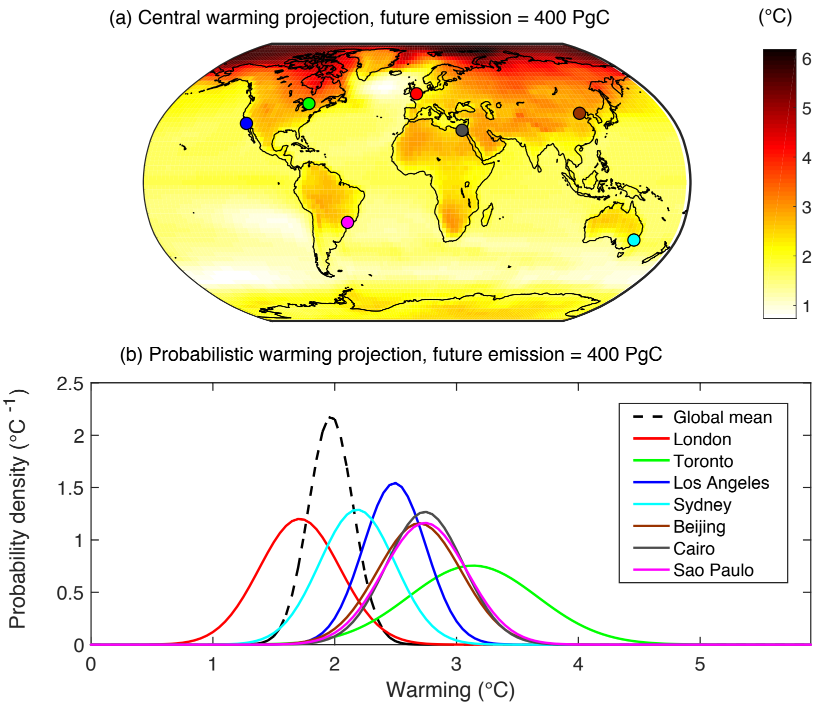

Figure 5: Warming projections when future emissions reach 400 PgC from the start of 2018. (a) The spatial distribution of the central warming projection. (b) The probability distributions of local warming for 7 locations (solid colour lines) and the global surface average (black dashed line). All warming projections given relative to the average temperature from 1850 to 1900. Global mean warming projected from the quadratic approximation to the history matched WASP ensemble (eqns. 3 to 6).